Structural Requirements of Sphingosine Molecules for Inhibition of DNA Primase: Biochemical and Computational Analyses†

Yasutomo Ito,§ Keiko Tamiya-Koizumi,¶ Yuuki Koide,‡,# Masako Nakagawa,# Tomohiko Kawade,# Atsushi Nishida,# Takashi Murate,⊥ Masaharu Takemura,¶ Motoshi Suzuki,¶ and Shonen Yoshida*,¶

Equipment Center for Research and Education, Laboratory of Cancer Cell Biology, Research Institute for Disease Mechanism and Control, School of Health Science, Nagoya University School of Medicine, Showa-ku, Nagoya 466-8550, Japan, Toa Eiyo Ltd., Omiya, Saitama, 330-0834, and Faculty of Pharmaceutical Science, Chiba University, Chiba 263, Japan

Received April 9, 2001; Revised Manuscript Received July 9, 2001

ABSTRACT: Using 28 chemically well-defined compounds containing D-*erythro*-sphingosine and its analogues, we analyzed structure−activity relationships for DNA primase inhibition. Biochemical studies demonstrated a positively charged amino group at C2 and a long aliphatic chain to be absolutely required for inhibition. Whereas C2-amino group is intact, sphingosine 1-phosphate was totally inactive. This result could be due to cancellation of positive charge of the amino group by the interaction with negatively charged C1-phosphate, since simulations with the software INSIGHT II showed these two groups to be close enough to interact. The hydroxyl group at C3 and *trans*-double bond at C4−C5 were also found to be important for the inhibition. Dehydroxylation of C3, as well as saturation or *cis*-conversion of the *trans*-double bond led to decrease of inhibitory activity. Despite saturation of the double bond, introduction of a hydroxyl group into C4 of dihydrosphingosine resulted in restoration of inhibition. Conversion of the double bond into a triple bond did not abolish but rather enhanced the inhibitory activity. Among sphingosine stereoisomers, the naturally occurring D-*erythro*-sphingosine proved to be the strongest inhibitor. To ascertain the contribution of the total conformation to the inhibition, especially of the long aliphatic chain, we constructed a 3D-quantitative structure−activity relationship model using the computer program Catalyst/HipHop on the basis of information described above. Analysis of the hypothesis model for active compounds revealed that the orientation of aliphatic chain, represented by the dihedral angle of C2−3−4−5, correlated well with the inhibition. Modifications such as deletion of the hydroxyl group at C3 or saturation of the C4−C5 double bond caused shifts in the dihedral angle of C2−3−4−5, with concomitant decrease in inhibitory activity.

The dominant sphingosine in mammalian cells is D-*erythro*-(2*S*,3*R*)-sphingosine,[1] which is an 18-carbon basic amine with a *trans*-double bond located between C4 and C5, and two hydroxyl groups located at C1 and C3 (designated as "sphingosine" hereafter). Sphingosine is a constituent unique to sphingolipids that may theoretically consist of approximately 60 000 molecular species according to the dramatic structural diversity in components, carbohydrate, fatty acid, and sphingosine (*1*). Endogenous free sphingosine also exists in cells, mainly originating from sphingomyelin hydrolysis. Since sphingosine is highly toxic to cells, it is metabolized rapidly to sphingosine 1-phosphate, and finally, to ethanolamine phosphate and palmitaldehyde. However, it has been also reported that sphingosine plays important roles in cell growth, differentiation, or oncogenesis through modulation of many enzyme activities (*2*−*4*). Especially, it inhibits protein kinase C and may affect a number of biological processes linked to protein kinase C-dependent pathways (*2*, *3*).

Although sphingomyelin exists predominantly in the plasma membrane, it is also found in the nucleus in association with chromatin (*5*−*7*) and nuclear matrix (*8*). Sphingomyelin hydrolyzing enzymes, sphingomyelinase (*7*, *9*, *10*) and ceramidase (*11*), also exist in the nucleus as well as the plasma membrane. Recently, we have shown that nuclear sphingomyelinase and ceramidase are induced prior

† This work was supported in part by a Grant-in Aid for Scientific Research from the Ministry of Education, Culture, Sports, Science and Technology of Japan.

* To whom correspondence should be addressed. Phone: 81 (52) 744-2453. Fax: 81 (52) 744-2457. E-mail: syoshida@tsuru.med.nagoya-u.ac.jp. Contact information for authors. (Y.I.) Equipment Center for Research and Education: Phone, 81 (52) 744-2407; Fax, 81 (52) 744-2408; E-mail, yitoh@tsuru.med.nagoya-u.ac.jp. (K.T−K., M.T., M.S., S.Y.) Laboratory of Cancer Cell Biology: Phone, 81 (52) 744-2453; Fax, 81 (52) 744-2457; E-mail, syoshida@tsuru.med.nagoya-u.ac.jp. (Y.K.) Toa Eiyo Ltd: Phone, 81 (48) 647-7971; Fax, 81 (48) 648-0078; E-mail, koide.yuuki@toaeiyo.co.jp. (Y.K., M.N.,T.K., A.N.) Chiba University: Phone, 81 (43) 290-2908; Fax, 81 (43) 290-3021; E-mail, nishida@p.chiba-u.ac.jp. (T.M.) Nagoya University School of Health Science: Phone, 81 (52) 719-1186; Fax, 81 (52) 719-1186; E-mail, murate@met.nagoya-u.ac.jp.

§ Equipment Center for Research and Education.

¶ Laboratory of Cancer Cell Biology.

‡ Toa Eiyo Ltd.

Chiba University.

⊥ Nagoya University School of Health Science.

[1] Abbreviations: sphingosine, D-*erythro*-sphingosine, D-*erythro*-*trans*-sphingosine, D-*erythro*-(2*S*, 3*R*)-sphingosine; 4,5-*cis*-sphingosine, D-*erythro*-*cis*-sphingosine; 4,5-t*riple*-sphingosine, D-*erythro*-t*riple*-sphingosine; dihydrosphingosine, D-*erythro*-dihydrosphingosine; araC, 1-beta-D-arabinofuranosylcytosine; HBA, hydrogen-bond acceptor; PosI, positive ionizable point; Hyd, hydrophobic point.

10.1021/bi010722i CCC: $20.00
Published on Web 08/29/2001

to apoptosis of rat hepatocytes after ligation of the portal vein branch, with concomitant increases in ceramide and sphingosine in nuclei (*11*). We have also found that sphingosine strongly inhibits DNA primase, an enzyme that is involved in both initiation and elongation of DNA replication (*12*). Mode of the inhibition of DNA primase by sphingosine and derivatives was shown to be competitive with template DNA but noncompetitive with dNTPs (*12, 13*). Concentration of sphingosine in nucleus of rat hepatocyte was varied from 3 to 10 μM before and after the induction by an apoptotic stimuli (*11*), ranging in the same order as those of K_i values described in the present study. The cytostatic/cytocidal effects of sphingosine and its analogues parallel DNA primase inhibition (*13*). These results suggest that DNA primase is one of the targets of sphingosine action. Interestingly, sphingosine induces apoptosis in the Bcl-2 overexpressing cells that are refractory to depletion of growth factor and treatments with methyl methane sulfonate, UV radiation, and X-rays (*14*).

In the present study, we have further analyzed the inhibition of DNA primase using sphingosine and 27 of its analogues, differing from each other in aliphatic chain length, residues at C1, C2, C3, and bond type between C4 and C5. Variation in inhibitory activity of these compounds clearly indicated that the amino group at C2, the hydroxyl group at C3, the double bond at C4−C5, and the length of the aliphatic chain are important for the inhibition. An important contribution of the total conformation for the inhibitory activity, especially of the orientation of aliphatic chain, was demonstrated by computer analysis of structure−activity relationships.

MATERIALS AND METHODS

Enzymes and Sphingolipids. DNA primase complexed with DNA polymerase α was purified from calf thymus by immunoaffinity column chromatography as described previously (*15*). Dihydrosphingosine, phytosphingosine, and *N*,*N*-dimethylsphingosine were purchased from Sigma Chemicals Co. (St. Louis, MO), and ceramide from bovine brain sphingomyelin, *N*-acetyl sphingosine, and *N*-octyl sphingosine from Matreya, Inc. (Pleasant Gap, PA). D-*erythro*-Sphingosine and all other analogues were synthesized and purified as described previously (*16*). Structures were verified by proton nuclear magnetic resonance and mass spectrometry. Poly dC was obtained from Amersham-Pharmacia Biotech UK Ltd. (Buckinghamshire, UK) and GTP from Yamasa Shoyu Co. Ltd. (Chiba, Japan). [α-^{32}P] GTP was purchased from Amersham-Pharmacia Biotech.

DNA Primase Assay. Activity of DNA primase was measured as described previously (*13*), with a standard reaction mixture (25 μL) containing 50 mM Tris/HCl (pH 7.5), 5 mM $MgCl_2$, 2 mM dithiothreitol, 400 μM [α-^{32}P] GTP (74 kBq), poly dC (16 μg/mL, 53.3 μM nucleotides), and 0.05 units of calf thymus DNA polymerase α-DNA primase complex. After incubation at 37 °C for 30 min, the reaction product was precipitated by ethanol with 1 mg of calf thymus DNA and subjected to 20% nondenaturating polyacrylamide gel electrophoresis. The radioactive spots at the top of gels, identified by a Hamamatsu DVS 3000 Image Analyzer system, were cut off and their radioactivities were determined with a liquid scintillation counter. To measure the inhibition, appropriate amounts of sphingosine and its analogues, stored in chloroform/methanol (2:1, v/v), were dried up under N_2 gas and suspended in water by ultrasonication. The suspended samples were preincubated with DNA polymerase α-primase complex for 15 min at room temperature, and then DNA primase activity was assayed as described above. The inhibition constant (K_i value) was calculated from the Dixon plot.

Computational Analyses. A 3D-quantitative structure−activity relationship model was constructed using the software package Catalyst 4.5 (Molecular Simulation Inc., San Diego, CA). All calculations were conducted on SGI Octane (R8000), running under the IRIX 6.5.4 operating system. A set of 18 inhibitors containing two hydroxyl groups and one amino group (compounds other than 15, 16, 17 in Table 3) was selected as a training set for Catalyst hypothesis model generation. A conformation model was calculated using the Best Quality method and an 18 kcal energy cutoff. The number of conformers generated for each molecule was limited to a maximum of 255. Since only few spans of inhibitory activities and a limited diversity of compounds were available, we generated the feature-based 3D-pharmacophoric alignment with Catalyst/HipHop. We focused on two hydroxyl groups at C1 and C3 (hydrogen-bond acceptor), one amino group at C2 (positive ionizable point) and four hydrophobic points on the aliphatic chain of sphingosine as features having putative chemical functions. To distinguish such functions from each other, the hypothesis model was generated using a set of highly constrained chemical features: positive ionizable (min: 1, max: 1), hydrogen-bond acceptor (min: 2, max: 2), and hydrophobic (min: 1, max: 1). A conformation model for each molecule was generated, and each conformer was examined for the presence of chemical features. Then, a 3D-configuration of each chemical feature common to the inputs was selected. All sets of generated conformers for compounds were ranked by scores, i.e., how well they could be superimposed on features in the hypothesis model (Fit value). By introducing biochemical data (actual K_i values), the generated hypotheses were further refined and used for the analyses. The estimated K_i for each compound was calculated from the Fit value. To investigate the structural factors supporting the most active conformation, dihedral angles of C1−2−3−4, C2−3−4−5, N−C2−3−O, and C3−4−5−6 were calculated.

The distances between the functional residues and the potential energy of compounds were calculated using the INSIGHT II software package. A model of D-*erythro*-sphingosine was built up manually and simple-minimized. Others were made on the basis of the minimized D-*erythro*-sphingosine model. The compounds were simulated with force field parameters based on the CVFF (consistent valence force field) (*17*). The grouped-based cut off, 0.95 nm for the van der Waals and 0.95 nm for coulomb interactions, were introduced. The temperature was set at 293 K. Calculations based on the simulation images were carried out using the INSIGHT II package (*18*).

RESULTS AND DISCUSSION

Inhibition of DNA Primase by Sphingosine Analogues. We classified 18 sphingosine analogues into five groups (Table 1), with respect to modification of the hydroxyl group at C1

Table 1: Inhibitory Effects of Sphingosine and Analogues on DNA Primase

Sphingosine and analogues [a]		DNA primase inhibition Ki (μM)[b]
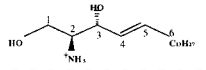	D-*erythro*-sphingosine	2.5
Group 1[c]		
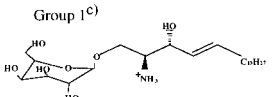	1-galactosyl sphingosine	3.2
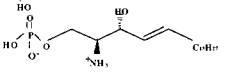	Sphingosine 1-phosphate	no inhibition
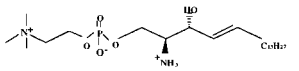	Sphingosylphosphocholine	1.9
Group 2[d]		
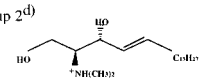	N,N-dimethyl sphingosine	2.5
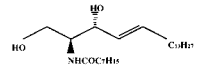	N-octyl sphingosine	no inhibition
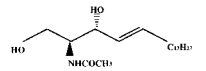	N-acetyl sphingosine	no inhibition
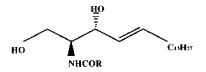	Natural ceramide	no inhibition
Group 3[e]		
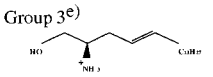	(R)-3-dehydroxy sphingosine	30
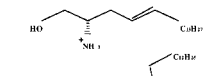	(S)-3-dehydroxy sphingosine	50
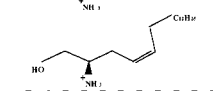	(R)-3-dehydroxy cis-sphingosine	25
Group 4[f]		
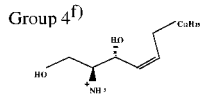	4,5-*cis*-sphingosine	10
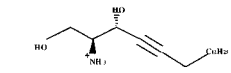	4,5-*triple*-sphingosine	1.8
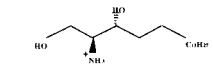	Dihydrosphingosine	15
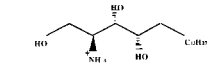	Phytosphingosine	3.0
Group 5[g]		
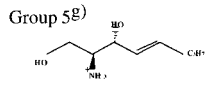	C8-sphingosine	no inhibition
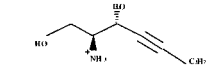	C8-4,5-*triple*-sphingosine	no inhibition
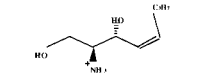	C8-4,5-*cis*-sphingosine	no inhibition

[a] The compounds in this table are all of D-erythro type except for group 3. [b] The values are mean of three experiments. [c] Analogues with reference to the C1 position of sphingosine. [d] Analogues with reference to amino residue at the C2 position. [e] Analogues dehydroxylated at the C3 position of sphingosine. [f] Analogues with reference to the C4 and C5 positions of sphingosine. [g] Short aliphatic chain analogues of sphingosine.

Table 2: Specificity of Sphingosine Stereoisomers Regarding DNA Primase Inhibition

	DNA primase inhibition K_i (μM)[a]			
stereoisomers	*trans*-double[b]	*triple*[b]	*cis*-double[b]	saturated (dihydro)[b]
D-*erythro*	2.5	1.8	10.0	15.0
L-*erythro*	12.7	8.3	8.2	
D-*threo*	8.3	11.2	5.7	
L-*threo*	8.0	11.2	4.2	16.2

[a] Values are means of three experiments. [b] Binding form between C4 and C5 of sphingosine stereoisomers.

(group 1), amino group at C2 (group 2), another hydroxyl group at C3 (group 3), the *trans*-double bond between C4 and C5 (group 4), and the aliphatic chain length (group 5) (Table 1). The importance of each modification for DNA primase inhibition was evaluated with regard to the inhibition constant (K_i). Inhibition of DNA primase by 19 compounds was measured as described in the Materials and Methods (also see ref 13), and the inhibition constants (K_i) of the analogues were obtained from Dixon plots.

In group 1, C1-modified compounds showed the strong inhibition that was comparable to that of sphingosine, except sphingosine 1-phosphate which entirely lost inhibitory effects. In group 2, where the amino group at C2 was modified, compounds lost the inhibitory activity, except for one modified with a dimethyl group. All of 3-dehydroxy sphingosine analogues in group 3 exhibited very low inhibition. In group 4, where the *trans*-double bond at C4−C5 was modified, compounds showed inhibitory effects with different potencies. One compound with triple-bonding (4,5-*triple*-sphingosine) inhibited DNA primase very strongly. One without a double bond (dihydrosphingosine) showed weak inhibition, but addition of hydroxyl group at C5 of this compound (phytosphingosine) fully restored inhibition capacity. Inhibition by an example with a *cis*-double bond was also weak. In group 5, the ones carrying much shorter aliphatic chains showed no inhibition.

Stereospecificity of DNA Primase Inhibition by Sphingosine. Sphingosine exists as four stereoisomers, i.e., combinations of D- and L-, and *erythro*- and *threo*-. To examine the stereospecificity of the inhibition of DNA primase by sphingosine, we measured the K_i values of the four stereoisomers, carrying the normal 4,5-*trans*-double bond. It was revealed that the D-*erythro*-form is the most potent inhibitor among the four (Table 2, the second column). Furthermore, we examined stereoisomers with a 4,5-triple bond and a 4,5-*cis*-double bond. With the triple bond compounds, it was also revealed that the D-*erythro*-form showed the most potent inhibition (Table 2, the third column). Therefore, the D-*erythro*-form is required for strong inhibition of DNA primase by sphingosine. In contrast, lowered inhibitory activity resulted from conversion of the 4,5 *trans*-double bond into a *cis*-configuration, was partly restored when it was converted to *threo*-isomers (Table 2, the fourth column).

Sphingosine has been shown to affect a number of enzymes (*19*−*26*) besides DNA primase. Among them, sphingosine inhibition of protein kinase C has been studied most extensively (*2*, *21*). For this, both a positively charged amine at C2 and a long aliphatic chain are also required (*21*, *26*). However, unlike the DNA primase inhibition, four stereoisomers of sphingosine similarly inhibit protein kinase

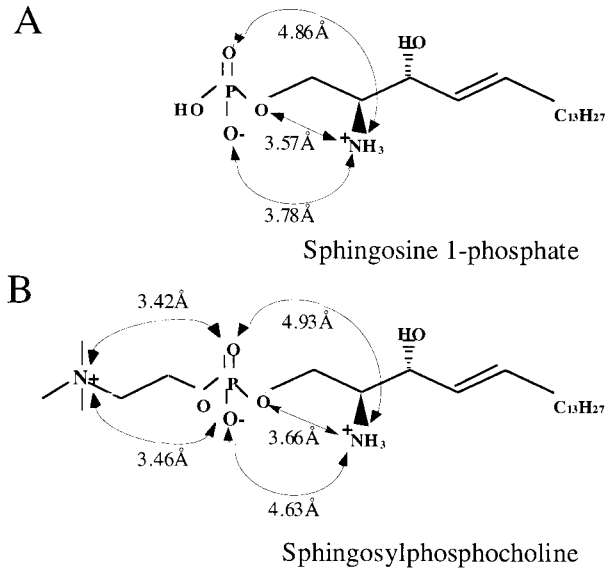

FIGURE 1: Intramolecular distances from C3-nitrogen to oxygen atoms. Computer simulations were carried out with 3D-conformation models of sphingosine 1-phosphate (A) and sphingosylphosphocholine (B) using the INSIGHT II software, as described in the Materials and Methods. The estimated distances are shown in the figure as the mean values of 100 calculations for each compound.

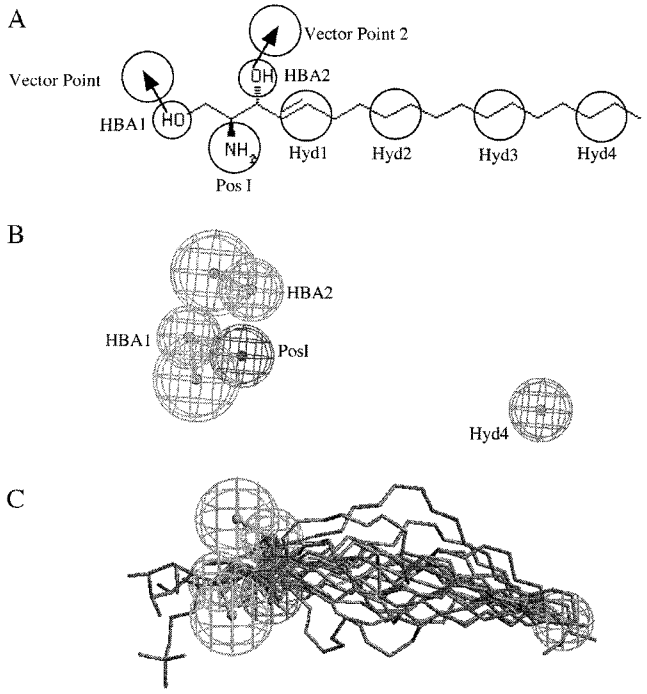

FIGURE 2: The construction of a 3D-quantitative structure−activity relationship model by Catalyst/HipHop. (A) The positions of used features that exhibit chemical functions in sphingosine molecule are shown, i.e., two hydroxyl groups at C1 and C3 (hydrogen-bond acceptors, HBA 1 and 2, with Vector Point 1 and 2), one amino group at C2 (positive ionizable point, PosI), and four hydrophobic points on the aliphatic chain (Hyd 1−4). They were used for the generation of the hypothesis model by Catalyst/HipHop. (B) A hypothesis model that consists of two HBA, PosI, two vector points and one Hyd at the end region of the aliphatic chain. This hypothesis model was selected after assessing the generated hypotheses with the biochemical data (actual K_i values). (C) Stereoview of alignment of compounds. Generated hypotheses for each compound (21 kinds, see Table 3) were aligned on the hypothesis model, and the best-fit conformation of each was selected as the active conformation.

C (*21*, *26*). Although a common mechanism that explains inhibitory effects of sphingosine on these enzymes has yet to be established, it is possible that these enzymes have a common structure that allows sphingosine binding.

The Importance of a Positively Charged Nitrogen at C2 for the Inhibition of DNA Primase. The important role of a positively charged C2-nitrogen for DNA primase inhibition is evident from the results for groups 1 and 2 (Table 1).

In group 1, modifications at C1 did not affect the inhibition with the exception of sphingosine 1-phosphate. This result suggests that the positively charged C2-nitrogen is essential for the inhibition of DNA primase and that in sphingosine 1-phosphate might be canceled by an intramolecular interaction with negative charge of the oxygen in the C1-phosphate. Therefore, we calculated the distances between the functional groups of group 1 compounds using the INSIGHT II software package, as depicted in Figure 1. In sphingosine 1-phosphate, the distance between the positively charged C2-nitrogen and the negatively charged oxygen of the C1-phosphate is near enough to allow electrostatic interaction, which could affect seriously the electric charge of the nitrogen atom at C2 and suppress its function with regard to DNA primase inhibition. In sphingosylphosphocholine, the oxygen of C1-phosphate is also negatively charged, but the distance to the nitrogen atom may be too far to make a stable interaction, because this phosphate group interacts with the positively charged choline at the other side of molecule (Figure 1). This may be the reason sphingosine 1-phosphate and sphingosylphosphocholine behave so differently. In 1-galactosyl sphingosine, the distance between the nitrogen and oxygen is nearer, but the oxygen does not have an electric charge and therefore is not so reactive as in a phosphate group.

The potential energy of each molecule in group 1 was calculated. Although the value for each compound fluctuated from trial to trial due to the molecular vibration, it was clear that the range of potential energy for sphingosine 1-phosphate was much lower (−35 to 2.5 kcal) than for other compounds with C1 modifications (group 1) such as sphingosylphosphocholine (197.4 to 233.6 kcal). The very low potential energy of sphingosine 1-phosphate may reflect the intramolecular interaction between the negatively charged oxygen of phosphate and the positively charged nitrogen (Figure 1).

In group 2, none of ceramides showed inhibitory effects. The C2-nitrogen of ceramide is not positively charged and does not serve as a proton acceptor, because the electron pair of the nitrogen is engaged in a resonance with the carbonyl group (*27*). *N*,*N*-dimethylsphingosine, the C2-nitrogen of which can serve as a proton acceptor, strongly inhibited DNA primase (Table 1). These results are consistent with the concept that the inhibition absolutely requires an amino group that is capable of protonation.

Orientation of Long Aliphatic Chain Influences the Inhibition of DNA Primase. Downstream of C2-nitrogen on the sphingosine molecule, there are other factors that influence inhibition. Deletion of the hydroxyl group at C3 of sphingosine (3-dehydroxysphingosine) largely diminished the inhibition (Table 1, group 3). Further, saturation of *trans*-double bond at C4−C5 (dihydrosphingosine) also reduced the inhibitory effect (Table 1, group 4). We postulated that these results reflect the varied orientation of the downstream aliphatic chain.

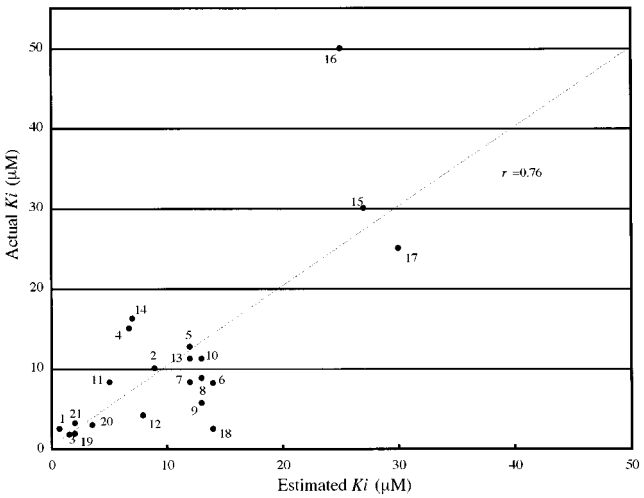

FIGURE 3: Correlation between the actual and estimated K_i. The estimated K_i for each compound was calculated from the Fit value, an index of the fitting level of each compound for the hypothesis model (Table 3). The correlation coefficient (r) is 0.76. Numbers for the points correspond to those for the compounds listed in Table 3.

To assess bulk conformation changes due to modifications, we analyzed whole molecules using Catalyst/HipHop software (see Materials and Methods). This program overcomes the difficulties in conformer selection and alignment of the flexible molecule such as with the compounds used here (*28*). It generates conformation models for each molecule using the Poling method that produces a good coverage of conformational space and defining the alignment rule focused on the chemical features (*29*−*32*). Such a feature-based 3D-pharmacophoric alignment (the hypothesis within Catalyst) is useful, especially when the 3D structure of the biological target (DNA primase in this study) is not available (*33*, *34*).

A set of 18 inhibitors containing two hydroxyl groups and one amino group was selected for generating the Catalyst hypothesis model. We chose two hydroxyl groups at C1 and C3, one amino group at C2 and one of fourhydrophobic points on the aliphatic chain as features having chemical functions (Figure 2A). After assessing the generated hypotheses with biochemical data (K_i values), the hypothesis model shown in Figure 2B was selected. Twenty-one components were analyzed sequentially using this hypothesis model to determine their alignment modes. Alignments of all 21 compounds to fit on the features at C1, C2, C3, and C17−18 of the hypothesis model are shown in Figure 2C. The fit value, an index that represents the fitting level of each compound for the hypothesis model, was used for calculation of the estimated K_i. A high level of correlation ($r = 0.76$) was demonstrated between the estimated K_i and the actual K_i (Figure 3) for each compound. These results indicate that the hypothesis model is sufficiently valid for analysis of the total conformation of each compound.

The conformation of whole molecule and the orientation of the aliphatic chain were represented by the dihedral angles of C1−2−3−4, C2−3−4−5, N−C2−3−O, and C3−4−5−6, obtained by the dynamics calculation on the basis of each active conformation (Table 3). Among these four angles, the dihedral angle of only C2−3−4−5 correlated well with the actual K_i (Figure 4). The dihedral angles of C2−3−4−5 of all 11 active compounds (actual $K_i < 10$ μM) were shown to be within the range of −65° to −125°, while those of 3-dehydroxy- or dihydro-analogues having much higher K_i values (Table 1) deviated greatly from this range (Table 3 and Figure 4). The C2−3−4−5 dihedral angle represents the orientation of the proximal region of aliphatic chain from C2 that is conjugated with an amino group. Therefore, the orientation of the aliphatic chain in the sphingosine molecule may also be an important factor for biological activity as a replication inhibitor.

It was remarkable that removal of the hydroxyl group at C3 (*R*-3-dehydroxy-sphingosine) largely diminished the inhibitory activity of sphingosine, in association with a dramatic change in the dihedral angle of C2−3−4−5 (by 108°, see Table 3). This is, to our knowledge, the first observation that the hydroxyl group at C3 plays an important role in maintaining conformation of the downstream aliphatic chain of a sphingolipid.

Table 3: Dihedral Angles of Sphingosine and Analogues in Their Active Conformations

sample number	compound	Cl−2−3−4[a]	C2−3−4−5[a]	N−C2−3−O[a]	C3−4−5−6[a]
1	D-*erythro-trans*-sphingosine	177.9	−121.1	176.6	179.7
2	D-*erythro-cis*-sphingosine	−177.4	−123.1	−180.0	−0.1
3	D-*erythro*-triple-sphingosine	176.1	n.d.[b]	176.3	14.8
4	D-*erythro*-dihydro-sphingosine	−179.8	−178.4	178.3	178.0
5	L-*erythro-trans*-sphingosine	−72.2	−93.5	−74.8	161.1
6	L-*erythro-cis*-sphingosine	−162.1	−64.9	−166.6	0.3
7	L-*erythro-triple*-sphingosine	−71.8	n.d.[b]	−70.4	−9.4
8	D-*threo-trans*-sphingosine	−55.6	−121.5	−167.7	−178.9
9	D-*threo-cis*-sphingosine	−58.3	−124.4	−168.6	−0.9
10	D-*threo-triple*-sphingosine	−53.0	n.d.[b]	−162.2	−17.5
11	L-*threo-trans*-sphingosine	−176.2	−78.5	−65.5	−174.1
12	L-*threo-cis*-sphingosine	−167.9	−100.9	−61.9	4.8
13	L-*threo-triple*-sphingosine	64.6	n.d.[b]	172.9	150.6
14	L-*threo*-dihydro-sphingosine	172.5	170.6	−74.8	166.9
15	(*R*)-3-deoxy-*trans*-sphingosine	−172.3	131.1	n.d.[b]	179.2
16	(*S*)-3-deoxy-*trans*-sphingosine	−174.4	115.5	n.d.[b]	−169.8
17	(*S*)-3-deoxy-*cis*-sphingosine	61.6	−177.6	n.d.[b]	−2.6
18	*N*,*N*-dimethyl sphingosine	55.2	−89.0	−169.9	169.6
19	sphingosylphosphocholine	179.4	−121.1	177.8	178.7
20	phytosphingosine	−84.5	−69.6	−78.8	−59.0
21	1-galactosyl sphingosine	171.4	−122.2	170.3	−178.7

[a] The carbon atoms of sphingosine are numbered as shown in Table 1. [b] Not determined.

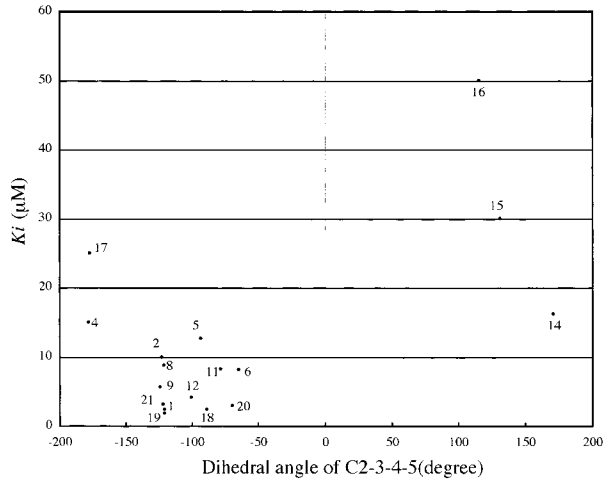

FIGURE 4: Dihedral angles of sphingosine and its analogues. Dihedral angles for C2−3−4−5 in the aliphatic chains of each compound (Table 3) were plotted (horizontal axis) against the actual K_i value (vertical axis). Numbers for the points correspond to those for the compounds listed in Table 3.

Effects of Length of the Aliphatic Chain. Analogues with short aliphatic chains were tested for inhibition of DNA primase. As shown in Table 1 (group 5), compounds carrying eight carbon aliphatic chains did not show any inhibition, even though the upstream portions were the same as for sphingosine or 4,5-*triple*-sphingosine. Therefore, in addition to the protonation of the C2-amino group and the orientation of aliphatic chain, the length of aliphatic chain is an important factor for the inhibition of DNA primase. In this connection, it has been reported that long-chain fatty acids inhibit DNA polymerase β, but shorter ones do not (*35*). Interestingly, fatty acids bind to the N-terminal 8-kDa domain of DNA polymerase β (*36*), which shares a significant homology with the 58-kDa subunit of DNA primase (*37*). This may indicate that the aliphatic long-chain of sphingosine binds to DNA primase through a similar mechanism as that operating between fatty acid and DNA polymerase β (*36*).

The conclusions deduced from the present study are as follows: (i) modification at C1 does not affect the inhibition, except with sphingosine 1-phosphate, where the intramolecular interaction between oxygen of C1-phosphate and C2-nitrogen may cancel the positive charge of nitrogen and suppress the function of the amino group; (ii) the positively charged amino group at C2 is absolutely required for inhibition, since a compound in which the amino group was conjugated with a carboxyl group (ceramide) showed no inhibition; (iii) the dihedral angle of C2−3−4−5, that determines the orientation of downstream aliphatic chain, is important for inhibitory function. Deletion of the C3-hydroxyl group or saturation of *trans*-double bond resulting in the reduction of the inhibitory activity accompanied by deviation of the angle; (iv) the length of the aliphatic chain is also an important factor for the inhibition, since compounds carrying short aliphatic chains did not show any inhibition.

Inhibition of DNA primase by sphingosine may block the progression of S phase by inhibiting both initiation and elongation of DNA replication, as observed in the inhibition of DNA polymerase α by aphidicolin (*38*) or araC (*39*). Resulted apoptosis may be implicated in the mechanism of cancer chemotherapy. In this context, the computer-assisted structural study of the inhibition by sphingosine presented here may provide a useful information to create a new candidate for anti-cancer compound.

ACKNOWLEDGMENT

The authors thank Mr. Seiichi Kobayashi of Ryoka Systems Inc. for his technical support with Catalyst. We also express our appreciation to Ms. Miwa Takahashi and Tazuko Tomita for their expert technical assistance.

REFERENCES

1. Ghidoni, R., Sala, G., and Giuliani, A. (1999) *Biochim. Biophys. Acta 1439*, 17−39.
2. Hannun, Y. A., and Linardic, C. M. (1993) *Biochim. Biophys. Acta 1154*, 223−236.
3. Igarashi, Y. (1997) *J. Biochem. 122*, 1080−1087.
4. Spiegel, S., and Milstien, S. (1995) *J. Membr. Biol. 146*, 225−237.
5. Spangler, M., Coetzee, M. L., Katyal, S. L., Morris, H. P., and Ove, P. (1975) *Cancer Res. 35*, 3131−3135.
6. Alesenko, A. V., Burlakova, E. B., & Pantaz, E. A. (1984) *Biokhimiia 49*, 621−628.
7. Albi, E., and Magni, M. P. (1997) *Biochem. Biophys. Res. Commun. 236*, 29−33.
8. Cocco, L., Maraldi, N. M., Manzoli, F. A., Gilmour, R. S., and Lang, A. (1980) *Biochem. Biophys. Res. Commun. 96*, 890−898.
9. Tamiya-Koizumi, K., Umekawa, H., Yoshida, S., and Kojima, K. (1989) *J. Biochem. 106*, 593−598.
10. Alessenko, A., and Chatterjee, S. (1995) *Mol. Cell. Biochem. 143*, 169−174.
11. Tsugane, K., Tamiya-Koizumi, K., Nagino, M., Nimura, Y., and Yoshida, S. (1999) *J. Hepatol. 31*, 8−17.
12. Simbulan, C. M., Tamiya-Koizumi, K., Suzuki, M., Shoji, M., Taki, T., and Yoshida, S. (1994) *Biochemistry 33*, 9007−9012.
13. Tamiya-Koizumi, K., Murate, T., Suzuki, M., Simbulan, C. M., Nakagawa, M., Takemura, M., Furuta, K., Izuta, S., and Yoshida, S. (1997) *Biochem. Mol. Biol. Int. 41*, 1179−1189.
14. Isogai, C., Murate, T., Tamiya-Koizumi, K., Yoshida, S., Ito, T., Nagai, H., Kinoshita, T., Kagami, Y., Hotta, T., Hamaguchi, M., and Saito, H. (1998) *Exp. Hematol. 26*, 1118−1125.
15. Tamai, K., Kojima, K., Hanaichi, T., Masaki, S., Suzuki, M., Umekawa, H., and Yoshida, S. (1988) *Biochim. Biophys. Acta 950*, 263−273.
16. Herold, P. (1988) *Helv. Chim. Acta 71*, 263−273.
17. *Discover 95.0/3.0.0 Forcefield Simulations User Guide*.
18. Rich, M. R., and Evans, J. S. (1996) *Biochemistry 35*, 1506−1515.
19. Mullmann, T. J., Siegel, M. I., Egan, R. W., and Billah, M. M. (1991) *J. Biol. Chem. 266*, 2013−2016.
20. McDonald, O. B., Hannun, Y. A., Reynolds, C. H., and Sahyoun, N. (1991) *J. Biol. Chem. 266*, 21773−21776.
21. Merrill, A., Jr., Nimkar, S., Menaldino, D., Hannun, Y. A., Loomis, C., Bell, R. M., Tyagi, S. R., Lambeth, J. D., Stevens, V. L., Hunter, R., et al. (1989) *Biochemistry 28*, 3138−3145.
22. Arnold, R. S., and Newton, A. C. (1991) *Biochemistry 30*, 7747−7754.
23. Davis, R. J., Girones, N., and Faucher, M. (1988) *J. Biol. Chem. 263*, 5373−5379.
24. Lavie, Y., and Liscovitch, M. (1990) *J. Biol. Chem. 265*, 3868−3872.
25. Jefferson, A. B., and Schulman, H. (1988) *J. Biol. Chem. 263*, 15241−15244.
26. Igarashi, Y., Hakomori, S., Toyokuni, T., Dean, B., Fujita, S., Sugimoto, M., Ogawa, T., el-Ghendy, K., and Racker, E. (1989) *Biochemistry 28*, 6796−6800.
27. Irmin, P. (1976) *Biochim. Biophys. Acta 455*, 433−451.
28. Guner, O. F. (2000) *Pharmacophore Perception, Development, and Use in Drug Design*, 69−84.
29. Smellie, A., Teig, S. L., and Towbin, P. (1995) *J. Comput. Chem. 16*, 171−187.

30. Smellie, A., Kahn, S. D., and Teig, S. L. (1995) *J. Chem. Inf. Comput. Sci. 35*, 285−294.
31. Smellie, A., Kahn, S. D., and Teig, S. L. (1995) *J. Chem. Inf. Comput. Sci. 35*, 295−304.
32. Greene, J., Kahn, S. D., Savoj, H., Sprague, P., and Teig, S. L. (1994) *J. Chem. Inf. Comput. Sci. 34*, 1297−1308.
33. Langer, T., and Hoffmann, R. D. (1998) *J. Chem. Inf. Comput. Sci. 38*, 325−330.
34. Palomer, A., Pascual, J., Cabre, F., Garcia, M. L., and Mauleon, D. (2000) *J. Med. Chem. 43*, 392−400.
35. Mizushina, Y., Yoshida, S., Matsukage, A., and Sakaguchi, K. (1997) *Biochim. Biophys. Acta 1336*, 509−521.
36. Mizushina, Y., Ohkubo, T., Date, T., Yamaguchi, T., Saneyoshi, M., Sugawara, F., and Sakaguchi, K. (1999) *J. Biol. Chem. 274*, 25599−25607.
37. Kirk, B. W., and Kuchta, R. D. (1999) *Biochemistry 38*, 7727−7736.
38. Murate, T., Kagami, Y., Hotta, T., Yoshida, T., Saito, H., and Yoshida, S. (1990) *Exp. Cell Res. 191*, 45−50.
39. Yoshida, S., Yamada, M., and Masaki, S. (1977) *Biochim. Biophys. Acta 477*, 144−150.

BI010722I